energies

MDPI

Article

Study on the Measurement Technique and Judgment Procedure of Ultrasonic Corona Imaging Equipment

Ja-Yoon Kang [1,2], Dong-Ju Chae [2], Young-Chae Mun [2], Ji-Man Park [2] and Bang-Wook Lee [3,*]

[1] Department of Mechatronics Engineering, Hanyang University, Ansan 15588, Republic of Korea; kangja@kesco.or.kr
[2] Electrical Safety Research Institute, Korea Electrical Safety Corporation, Wanju 55365, Republic of Korea; chaedju@kesco.or.kr (D.-J.C.); ycmun@kesco.or.kr (Y.-C.M.); jmpark@kesco.or.kr (J.-M.P.)
[3] Department of Electronic Engineering, Hanyang University, Ansan 15588, Republic of Korea
* Correspondence: bangwook@hanyang.ac.kr; Tel.: +82-31-400-4752

Abstract: Corona discharge is a phenomenon wherein gas on the surface of electrical equipment is ionised. Severe ionisation can lead to insulation breakdown and cause equipment damage. Consequently, non-contact portable devices are employed to detect corona discharge in real time while the electrical equipment is pressurised. Recently, several devices capable of visualising corona discharge phenomena occurring in the ultrasonic region have been developed. However, these devices are primarily used for scanning purposes to verify the occurrence of partial discharge, as detailed guidelines for operating the equipment in real-world field conditions are yet to be established. Therefore, this study proposes a measurement technique for utilising ultrasonic corona imaging diagnostic equipment in the field. This technique involves the use of corona discharge electrodes and aged epoxy insulator samples. First, the performance of the ultrasonic corona imaging diagnostic equipment based on environmental conditions was evaluated by varying the distance, frequency, temperature, and humidity using the corona discharge electrodes. Then, parallel measurements were conducted with a high-frequency current transformer sensor on epoxy insulator samples subjected to simple ageing, cracking, and partial surface damage, and the results were analysed. Finally, an efficient measurement technique, including equipment operation procedures, was proposed by integrating the measurement results.

Keywords: corona discharge; epoxy insulator; ultrasonic corona imaging diagnostic equipment; high-frequency current transformer sensor

Citation: Kang, J.-Y.; Chae, D.-J.; Mun, Y.-C.; Park, J.-M.; Lee, B.-W. Study on the Measurement Technique and Judgment Procedure of Ultrasonic Corona Imaging Equipment. *Energies* **2023**, *16*, 5529. https://doi.org/10.3390/en16145529

Academic Editors: Junhao Li and Xutao Han

Received: 8 June 2023
Revised: 13 July 2023
Accepted: 18 July 2023
Published: 21 July 2023

1. Introduction

Partial discharge can be classified depending on the type of discharge that occurs on the surface, conductor, or interior of electrical equipment. Because its occurrence causes thermal, mechanical, chemical, and structural changes, the insulation performance of electrical equipment gradually weakens, causing accidents [1–4]. Therefore, early detection of partial discharge is crucial to prevent accidents. However, early symptoms of partial discharge are intermittent and difficult to detect without real-time monitoring. Furthermore, partial discharge occurs only when the equipment is in operation; therefore, non-contact portable devices have been used for uninterrupted state inspections. Partial discharge generates ultraviolet (UV) and visible light emissions, noise, a rise in local temperature, chemical species, and current pulses [5]. Although portable devices have been developed using non-electrical technologies, such as ultrasound, UV, and infrared sensing, non-electrical devices exhibit a higher error rate in the measurement results compared to electrical devices, owing to surrounding noise and measurement techniques. Therefore, they are utilised as scanning devices. However, simple scanning for corona discharge cannot justify the unconditional shutting down and maintenance of operational equipment considering it could result in significant losses and cause significant damage owing to production equipment shutdowns;

conversely, in households, frequent power outages can cause inconvenience, considering no established guidelines exist for assessments and measurement techniques when using the equipment. Therefore, the availability of such technical criteria can ensure economical maintenance using scanning devices by determining the condition as per the condition of the equipment: Good, caution, and abnormal.

Among the currently employed non-contact devices, ultrasonic detectors, infrared cameras, and UV imaging equipment are the most widely used. Ultrasonic detection technology utilises sensors to locate and analyse signals directly from the areas where sound waves are generated. However, ultrasonic detection technology can be time-consuming when determining the precise location of the occurrence. Alternatively, certain methods have been proposed for diagnosis by directly installing devices on equipment, such as Gas Insulated Switchgear and transformers [6–8]. The method using an infrared camera involves comparing thermal points in the surroundings to detect abnormal reactions. However, it provides relative values, making it impossible to accurately determine the cause of the occurrence. UV imaging equipment offers the advantage of visualising UV rays detected by sensors in specific locations as images, rendering it intuitive. However, significant noise due to sunlight in outdoor installations and a lack of reliable measurement techniques for determining severity restrict its applications. Various studies have been conducted to determine risk levels considering factors such as distance-related gain values and criteria based on the characteristics of UV rays represented as images [9–15].

Recently, equipment combining ultrasonic and imaging technology to visualise corona discharge phenomena has been developed. In contrast to previous methods, the use of sound waves enables the immediate visualisation of images, thereby allowing users to detect the accurate location of sound wave occurrence, similar to when UV imaging equipment is used, thereby reducing the diagnostic time. Additionally, as ultrasonic imaging equipment is portable, measurements can be performed conveniently on any target. Moreover, in contrast to the use of other technologies, by using sound waves, quantitative results in units of decibels can be obtained. This technology has recently been commercialised; however, similar to the cases of other devices, research on the guidelines and measurement techniques for reliable phased assessment is insufficient. We assume that ultrasonic imaging equipment is more likely to provide intuitive judgement criteria compared to other technologies. Therefore, if the assessment criteria are applied in the field, accidents can be prevented. Furthermore, economically efficient maintenance can be achieved as the results are more substantiated than those obtained previously.

Considering the abovementioned reasons, this study aimed to develop a criterion using ultrasound imaging equipment by investigating the measurement techniques and phased assessment criteria to determine corona discharge assessment guidelines for ultrasonic imaging equipment. Electric power facilities have different facility structures, environments, and inspection conditions for each installation location, making it impossible to perform an inspection under the same measurement conditions as those in the field. Therefore, it is necessary to set a standard measurement condition and correct the result value according to the condition variable. When considering a site, condition variables include distance, frequency, temperature, and humidity. For a reliable criterion, the characteristics that change when corona discharge is measured using ultrasonic imaging equipment according to the variables were analysed. Additionally, because ultrasound is a non-electrical measurement method and uses a physical element that is different from the existing electrical measurement method, the shape and characteristics of the obtained result can be different. Therefore, this study compared the measurement results under the same conditions targeting a high-frequency current transformer (HFCT), which has been studied extensively and is reliable. By experimenting with epoxy insulators with various defects, the correlation was analysed by comparing the image and phase-resolved partial discharge (PRPD), the result of ultrasound imaging equipment, with PRPD and Pulse spectrum, the result of HFCT.

The remainder of this paper is organised as follows. Section 2 summarises the measurement techniques using a needle–plane electrode system to derive reliable measurement results. Section 3 describes the determination of phased assessment criteria by accelerating the ageing of the epoxy insulator and categorisation based on the defect type. For reliable criterion analysis, we simultaneously conducted measurements using an HFCT, which has been extensively researched as an electrical device among the various partial discharge detection technologies. Section 4 reviews the issues to be addressed to devise assessment criteria based on the experimental results. Finally, Section 5 summarises the conclusions and proposes future research directions.

2. Measurement Techniques for Obtaining Reliable Measurement Results

In contrast to electrical sensors, the implications of the measured values in non-electrical sensors change depending on the natural environment and measurement conditions. For example, in the case of ultrasonic waves, the severity of the measurement target changes with the distance, even when the values are the same. Therefore, it is necessary to analyse the results based on the measurement conditions to ensure accurate assessment irrespective of differing conditions. Therefore, we simulated corona discharge using a needle–plane electrode system and analysed the variations of the results according to the distance, measurement frequency, temperature, and humidity. Figure 1 shows photographs of the needle–plane electrode system and ultrasonic imaging equipment used in the experiment. The measurement conditions were maintained during the experiment. The distance between the needle and plate was 1.5 cm, and the applied voltage was 10 kV. A Fluke ii910 ultrasonic imaging system was utilised in this study. The acoustic camera comprised 64 microphones operating in the 2–100 kHz range. The acoustic levels were measured in units of decibels, and the screen displayed different colours based on the acoustic levels.

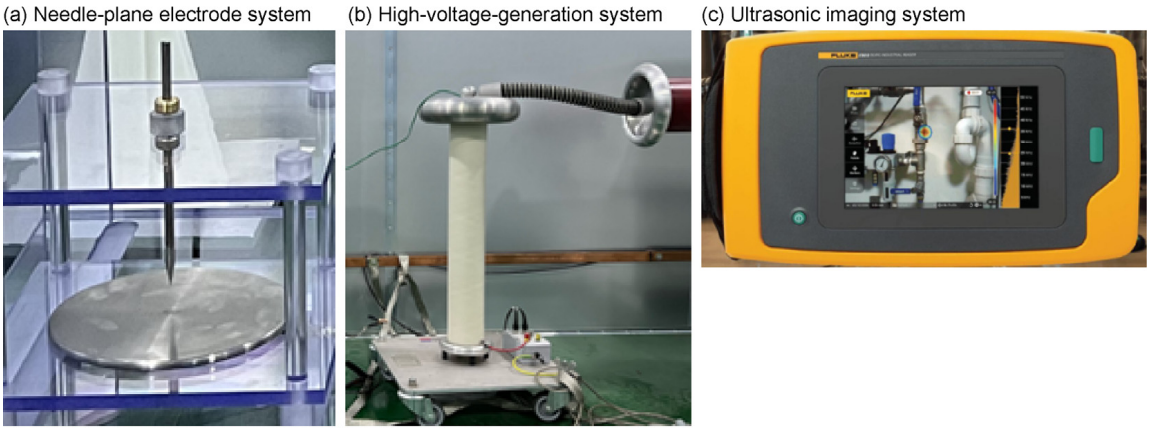

Figure 1. Needle–plane electrode system and ultrasonic imaging equipment. (**a**) Needle–plane electrode system; (**b**) high-voltage-generation system; (**c**) ultrasonic imaging system.

2.1. Measurement Conditions: Distance

Although ultrasonic waves exhibit the same properties as sound waves, a distinguishing feature of ultrasonic waves is that their size attenuates with distance. While certain differences are observed depending on the sound wave frequency, temperature, and humidity, the attenuation rate based on distance is generally determined theoretically as:

$$S_2 = S_1 + 20\log\frac{D_1}{D_2}, \quad (1)$$

where D_1 and D_2 are the distances from the sound source to measurement positions 1 and 2, respectively, and S_1 and S_2 are the sound wave sizes at measurement positions 1 and 2, respectively. Using Equation (1), when the measurement distance changes from 1 to 2 m and 1 to 3 m, the size of the sound waves presumably decreases by 6.02 ($20\log\frac{1}{2} \approx -6.02$)

and 9.54 dB ($20\log\frac{1}{3} \approx -9.54$), respectively. To verify whether Equation (1) can be applied during partial discharge measurements, we utilised a needle–plane electrode system that could repeatedly simulate the partial discharge at a relatively similar level as the source of the partial discharge. Under the same conditions, the measurement distance was set to 1, 2, 3, 4, and 5 m, and 15 repeated measurements were performed. Figure 2 shows the measurement data.

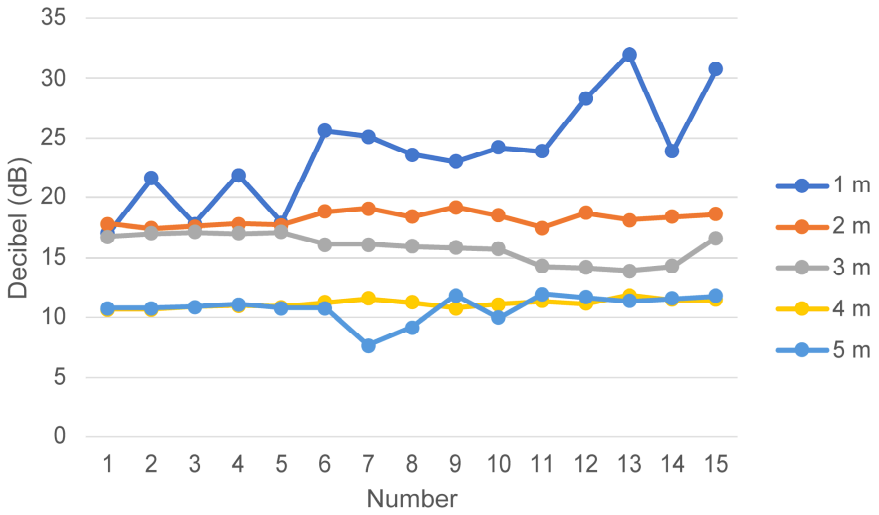

Figure 2. Results of the repeated measurements depending on the distance.

As shown in Figure 2, different decibel levels were obtained for the same distance. The measured decibel values were different even at the same distance owing to the aperiodic nature of the partial discharge. Therefore, the average value was calculated through repeated measurements. As the distance increased, the range and average value decreased. Figure 3 presents a comparison of the decrease in the theoretical (obtained using Equation (1)) and experimental values as the distance increased from the 1 m base. Although certain discrepancies were observed between the two sets of values, the values were similar, with error rates of 8.6%, 16.9%, 3.8%, and 7.7%. Therefore, measurements cannot be conducted using high-voltage equipment in switchgear at a fixed position for assessment, considering the structure varies with the location. However, the experiment confirmed that the decibel levels can be estimated for desired distances using values measured at arbitrary distances.

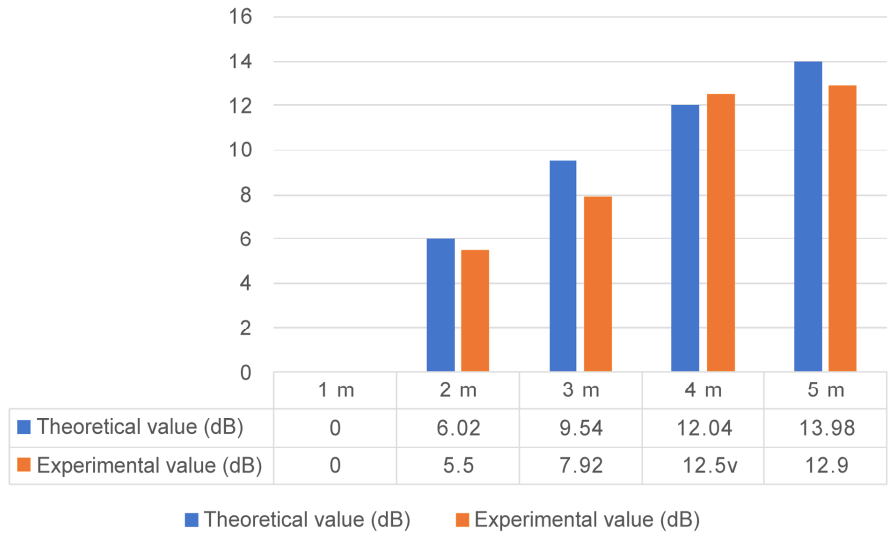

Figure 3. Decrease in the decibel values as the distance increased from the 1 m base: Theoretical and experimental results.

2.2. Measurement Conditions: Frequency

Ultrasonic waves generated by corona discharge are irregularly distributed across the entire ultrasonic frequency range; however, previous research results showed that their distribution is relatively dense in the 30–50 kHz frequency band [6]. This characteristic differs from the frequency distribution pattern of general noise and serves as the basis for selecting the frequency band for measurements when detecting corona and most partial discharges using ultrasound. At actual corona discharge inspection sites, noise signals from air conditioners, fans, lights, and uninterruptible power supplies, as well as their reflected waves, are mixed. To detect the ultrasonic waves generated by partial discharge at such sites, frequencies above a certain level must be observed within the ultrasonic band. Consequently, the measurement frequency must be experimentally analysed for corona discharge detection.

The equipment used for measurement can detect ultrasonic waves within a selected range of 5–20 kHz, covering a 2–100 kHz frequency band. The same needle–plane electrode system and equipment used for the distance experiment were employed in this study. The data obtained for the 5–100 kHz range were divided into 19 different ranges for analysis, from 5–10 to 95–100 kHz. Figure 4 shows the amounts and ratios of measured data collected with 575 data points in each range. The standard for the measured data was determined based on the data identified as those of the corona discharge through PRPD patterns. Here, 88.5% of the data were measured in the 25–45 kHz range.

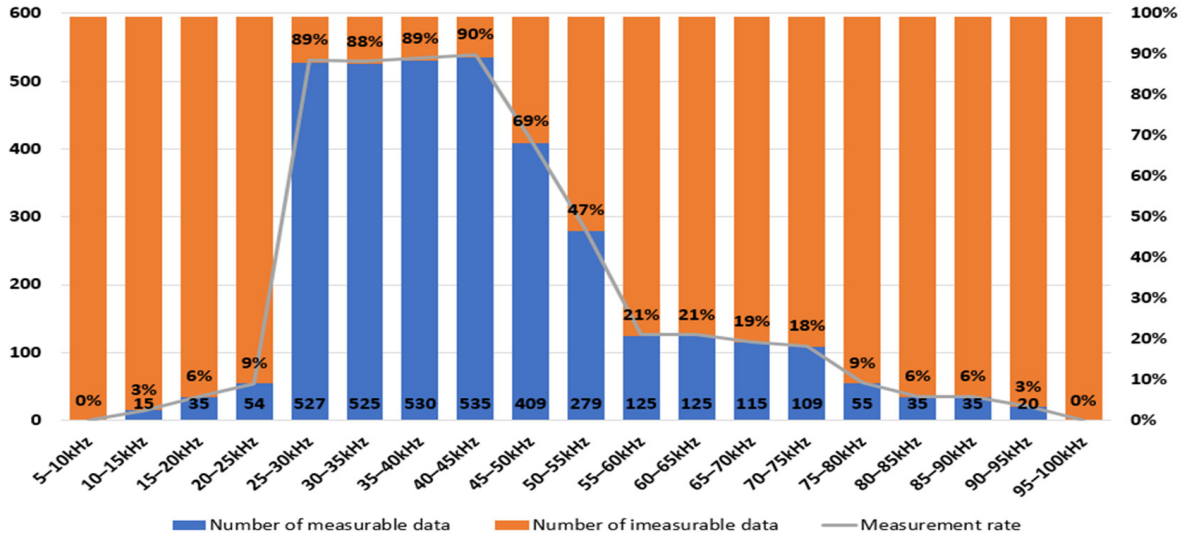

Figure 4. Analysed data depending on the frequency range.

Figure 5 shows the average values of valid data measured according to the distance and frequency. Considering the trend of decreasing measurement values with increasing distance, measurements performed within the 25–40 kHz range should be accurate. In previous studies, partial discharge components appeared at approximately 30–50 kHz [6]. Furthermore, considering the experimental results of the present study, the 30–40 kHz range was estimated as the optimal frequency range for measurements at short distances.

2.3. Measurement Conditions: Temperature and Humidity

Partial discharge varies in occurrence and severity depending on environmental factors such as temperature and humidity, even when using the same equipment. For example, the phenomenon of partial discharge occurring even under the same equipment operating conditions differs between indoor and coastal environments. According to the results in [16], the onset voltage decreases as temperature and humidity increase.

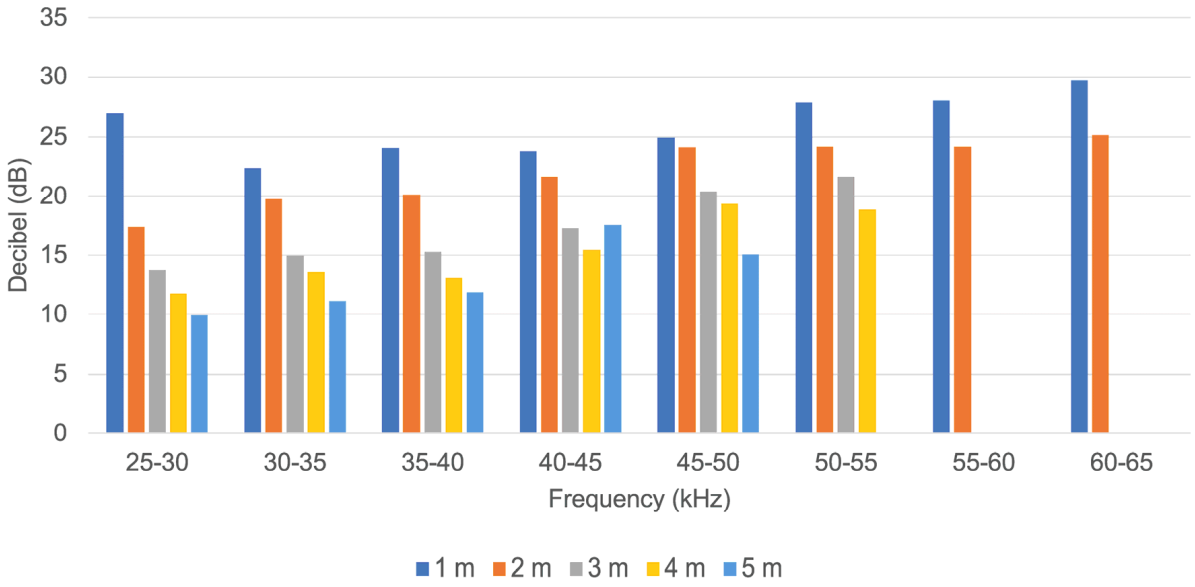

Figure 5. Measurement results according to the measurement frequency range (by distance).

Experiments were conducted to determine whether similar characteristics appeared in ultrasonic wave measurements during summer and winter environments. The summer conditions were 23 °C and 83% humidity, whereas the winter conditions were 6 °C and 51% humidity. Figure 6 summarises the corona discharge measurement results under the summer and winter conditions. The results are presented in terms of frequency, and corona discharge was consistently detected and measured in the 35–40 kHz range. Based on this frequency range, higher decibel levels were measured under summer conditions with high temperatures and humidity. Additionally, we confirmed a decrease in the effective frequency range measured in winter. Therefore, the experimental results confirmed that the characteristics of corona discharge occurrence due to temperature and humidity can be detected using ultrasonic wave measurements.

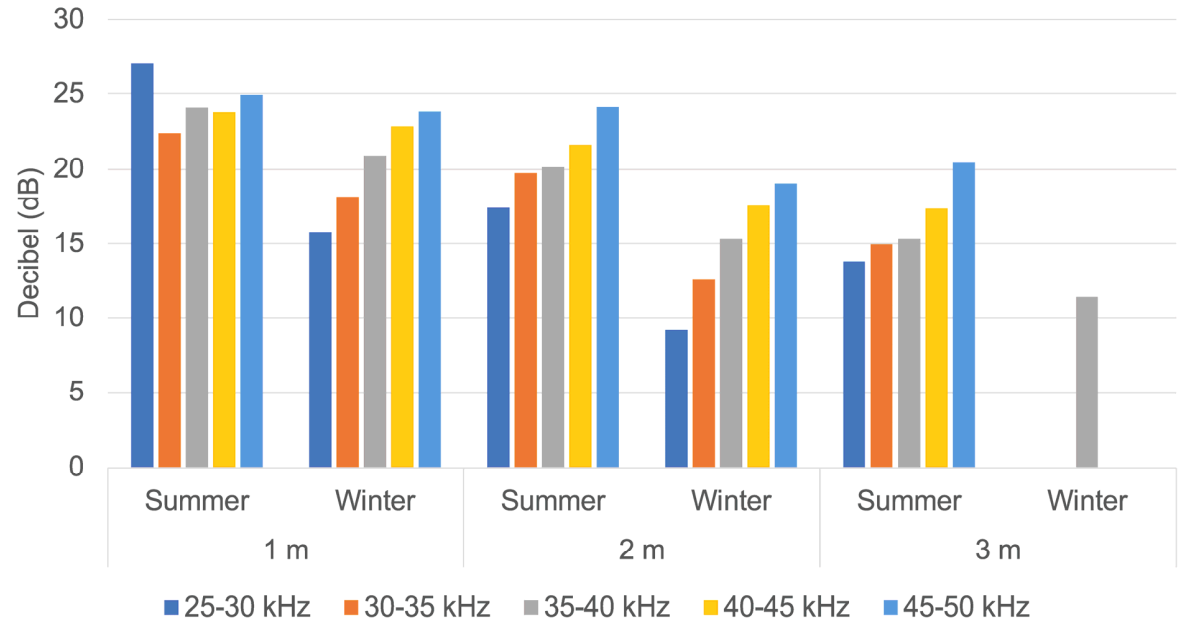

Figure 6. Corona discharge measurement results obtained under summer and winter environmental conditions.

3. Analysis of the Experimental Results According to Defect Types of Specimens to Determine Phased Assessment Criteria

Next, experiments were conducted by dividing the same samples into different defect types to acquire data to determine the phased assessment criteria. Epoxy insulators, which are commonly employed to maintain insulation gaps in switchgear, were utilised for the samples. The phased assessment criteria should be detected according to the sample type because accidents can occur owing to insulation degradation from partial discharge. In this study, epoxy insulators used for 20 years were collected, and their ageing was accelerated using a temperature and humidity chamber. Three types of defects were considered: Simple ageing caused by the service life, crack occurrence caused by the environment, and damage caused by external physical forces. Figure 7 shows photographs of samples categorised based on the defect type. Figure 7a depicts the sample subjected to simple ageing with three cycles of two weeks of UV exposure and two weeks of exposure to high temperatures and humidity. Figure 7b presents the cracked sample subjected to two weeks of UV exposure and two weeks of thermal cycling (three cycles). Figure 7c shows the sample damaged on one side that was subjected to accelerated ageing under the same conditions as those used to obtain the sample shown in Figure 7a. Table 1 summarises the detailed conditions of the accelerated ageing test.

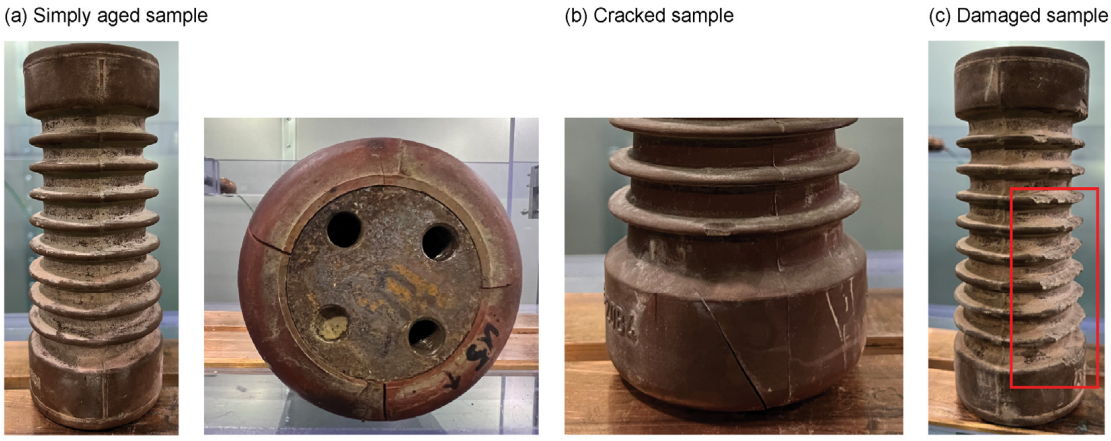

Figure 7. Samples used in the experiment. (**a**) Simply aged sample; (**b**) cracked sample; (**c**) damaged sample.

Table 1. Detailed conditions of the accelerated ageing test.

Test	Detailed Conditions		
UV	Light	1.55 W/(m^2·nm), 70 °C	
	Condensation	Dark phase, 50 °C	
Thermal cycle	High temperature	100 °C (1 h)	Temperature change 4 °C/min
	Low temperature	−30 °C (1 h)	
High temperature/humidity	85 °C/80% R.H.		

For the simple ageing samples, the overall colour became darker because of UV exposure, and indications of surface corrosion were observed. For the cracked samples, thermal expansion occurred owing to the influence of the thermal cycle, resulting in cracks near the insulator connection area. Meanwhile, the damaged samples were subjected to the same conditions as the simple ageing samples and differed in the occurrence of damage to one side.

Experiments were conducted through simultaneous measurements with an HFCT and ultrasonic imaging equipment, which has been extensively researched and is used

to measure partial discharge via electrical methods. The HFCT was selected because it is a highly reliable technology that can directly detect electrical signals and determine the presence, type, and severity of partial discharge. PRPD patterns and pulse spectra were measured using the HFCT and compared with the PRPD and decibel level measurements obtained using ultrasonic imaging equipment. To minimise noise during the HFCT installation, only the ground and high-voltage input wires were connected on both sides of the epoxy insulator. Figure 8 shows the high-voltage equipment test jig and HFCT equipment utilised in the experiment.

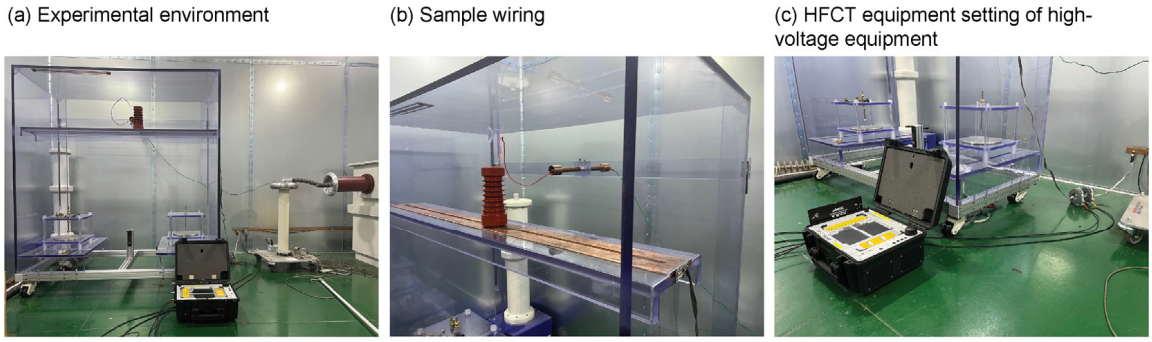

Figure 8. Photographs of the experimental environment. (**a**) Experimental environment; (**b**) sample wiring; (**c**) HFCT equipment setting of high-voltage equipment.

Figure 9 shows the PRPD patterns measured by the HFCT when a voltage was applied to the epoxy insulator, resulting in partial discharge. A mixed pattern of corona and floating discharges was obtained, where pulses were concentrated only in one phase. The PRD patterns were seen to be concentrated at approximately −10 pC at approximately 90 degrees out of phase (Figure 9a), −25 pC at approximately 30 degrees of phase (Figure 9b), and −30 pC at 45 degrees (Figure 9c).

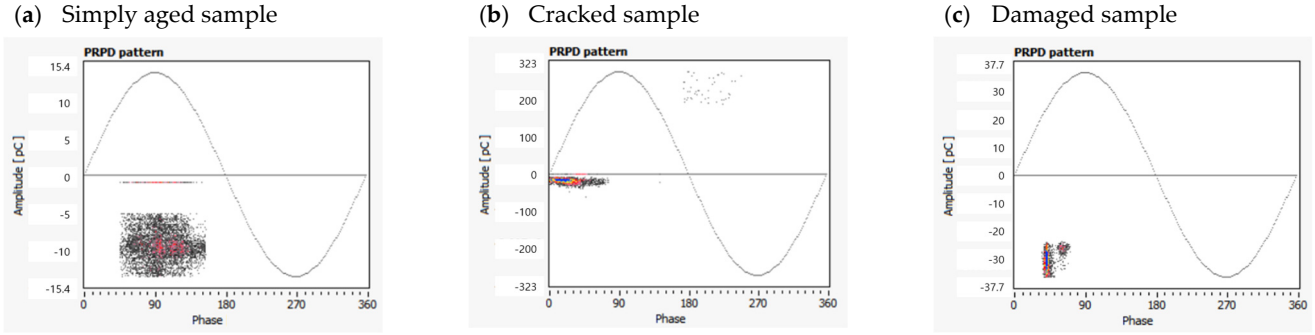

Figure 9. PRPD patterns obtained using the HFCT for different defect types. (**a**) Simply aged sample; (**b**) cracked sample; (**c**) damaged sample.

Figure 10 shows images of the simply aged and cracked samples obtained using ultrasonic imaging equipment. As a result of measurement at the centre of 40 kHz, ultrasonic waves were generated at the connection part in the same way. However, it was not possible to secure the PRPD pattern because the ultrasonic wave judged as partial discharge was not measured.

Figure 11 shows the measurement results of the damaged sample obtained using ultrasonic imaging equipment. Here, ultrasonic waves were generated at the connection area, and a PRPD pattern was obtained with the measured 30 decibel levels. In the case of the PRPD pattern, pulses were concentrated around 90 degrees. Similar to that observed for the PRPD pattern obtained using the HFCT, pulses occurred only in one phase in the ultrasonic PRPD pattern. The difference between HFCT and ultrasonic PRPD is that the

PRPD of HFCT is negative, whereas ultrasonic PRPD is positive, and only positive values were used in this study owing to the characteristics of ultrasonic measurement.

(**a**) Simply aged

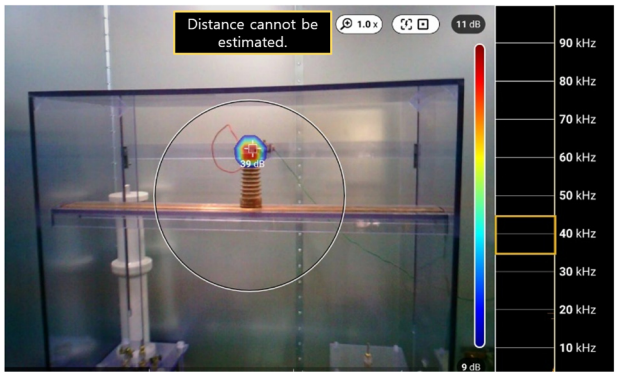

(**b**) Cracked samples obtained using ultrasonic imaging equipment

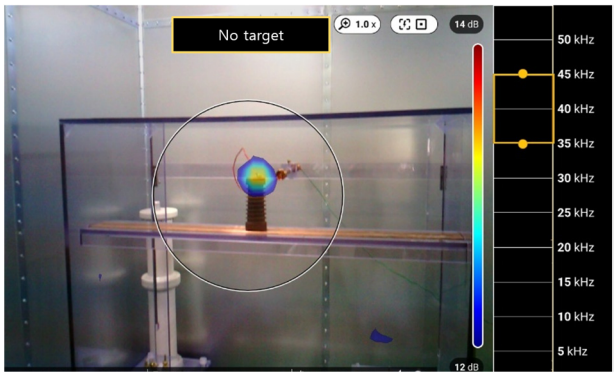

Figure 10. Images of (**a**) simply aged, (**b**) cracked samples obtained using ultrasonic imaging equipment.

(**a**) Measured image of the damaged sample

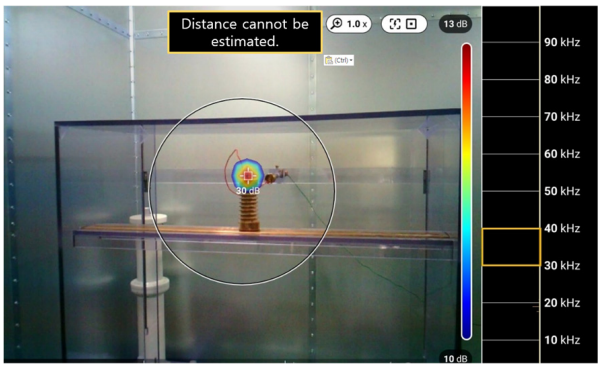

(**b**) Ultrasonic PRPD pattern of the damaged sample

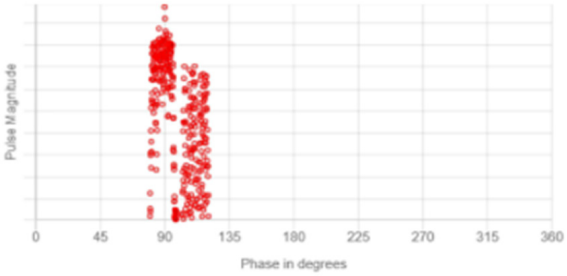

Figure 11. Measurement results for the damaged sample obtained using ultrasonic imaging equipment. (**a**) Measured image of the damaged sample; (**b**) ultrasonic PRPD pattern of the damaged sample.

According to the defect type, analysis of the graphs in Figure 9 yielded values of 9, 27, and 32 pC for the simply aged, cracked, and damaged samples, respectively. These results indicate that the severity of partial discharge increases in the presence of external impacts, such as cracks or damage, compared to that observed for simple ageing with usage. Moreover, the measured PRPD patterns resembled corona discharge patterns, thereby confirming the occurrence of partial discharge. However, when measured using ultrasonic imaging equipment, corona discharge was detected and measured for only the damaged sample. Despite the occurrence of partial discharge similar to that measured by HFCT, in ultrasonic PRPD, the results were obtained based on the actual measurements rather than the difference in the severity of the partial discharge. To analyse the cause of this difference, the pulse spectrum of HFCT was examined. Figure 12 presents the pulse spectrum analysis results for each defect type.

In the pulse spectrum analysis results, a spectral peak was observed at approximately 0 Hz and 10 MHz in the frequency band for the simply aged sample. In the cracked sample, pulses were generated around 0 Hz and 20 MHz, and pulse values around 0 Hz were measured to be larger. In the damaged sample, a larger value was seen at a higher frequency than in the cracked sample. In this sample, a relatively large pulse occurred only around 20 MHz. The maximum pulse values in the high-frequency region were measured as (a) 0.16 mV (Figure 12a), (b) 0.6 mV (Figure 12b), and (c) 0.9 mV (Figure 12c) for the three samples. This confirms that the more severe the partial discharge, the larger the pulse occurring in the high-frequency region.

(**a**) Simple ageing

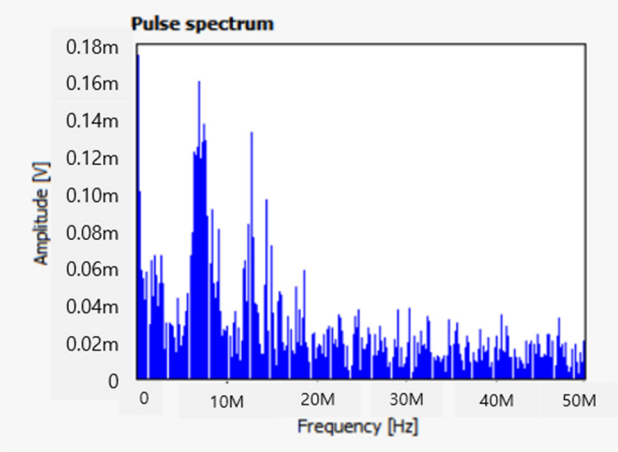

(**b**) Cracked

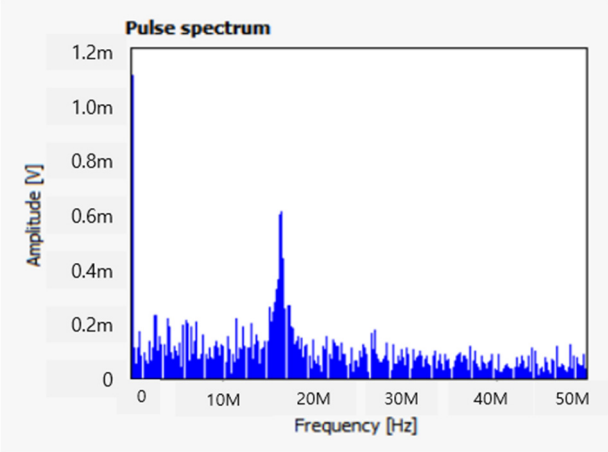

(**c**) Damaged

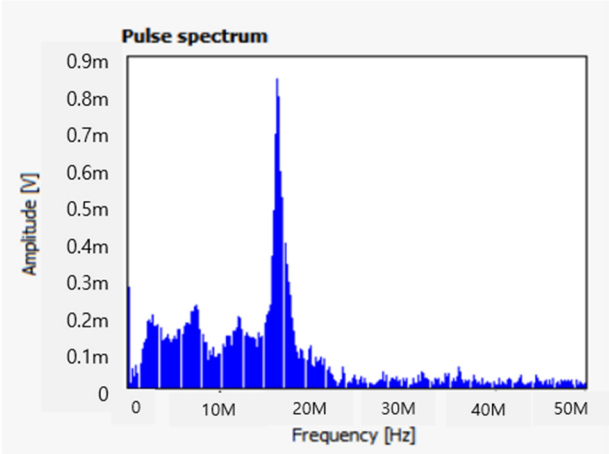

Figure 12. Pulse spectra for different defect types. (**a**) Simple ageing; (**b**) cracked; (**c**) damaged.

In particular, the highest pulse value occurred in the low-frequency band of approximately 0 Hz for the simply aged and cracked samples. The damaged sample was the most significant difference among the three samples, considering pulse values in the high-frequency range. For the simply aged and cracked samples, only ultrasonic waves were generated and corona discharge was not detected, as shown in Figure 10, because the pulse value in the low-frequency band was higher than that in the high-frequency range.

Finally, when comparing and analysing only the data for the high-frequency range, the maximum pulse value gradually became less distinct in the order of the damaged, cracked, and simply aged samples compared with the other pulse values. HFCT is a distinct partial discharge measuring device, which provides highly sensitive measurement results. Notably, the purpose of using the non-contact ultrasonic measuring equipment was facile detection using a portable unit, i.e., a compact device. Consequently, we expected the sensitivity of the measured waveforms to be lower than that obtained using the HFCT. Therefore, we anticipated the pulse value gap in the ultrasonic-measured pulse spectrum to shrink, which was assumed to be a reason for not detecting the corona discharge. This is because when actual imaging was conducted, partial discharge was detected in real time; however, during the time of saving the data, partial discharge was not detected, resulting in failure (Figure 10b).

A comparative analysis of the measurement results obtained using the HFCT and ultrasonic imaging equipment revealed that under identical conditions, the ultrasonic imaging equipment failed to detect partial discharge despite the actual occurrence of partial discharge. It is concluded that the ability to detect partial discharge is relatively

unaffected by variations in equipment resolution. However, although the equipment cannot detect partial discharge owing to issues related to the resolution or algorithm, the high-frequency band in Figure 11 indicates the generation of ultrasonic waves. This finding can be considered an initial indication of partial discharge, although not severe. By collecting and analysing data through such experiments, we expect that the applicability and utility of the non-contact partial discharge detection equipment can be considerably increased.

4. Discussion on the Assessment Criteria Based on the Experimental Results

This study established the criteria for assessing the corona discharge detection results obtained using ultrasonic imaging equipment. Experiments were conducted on two aspects required to devise the criteria. First, we performed experiments to understand the correlation between the obtained results according to the measurement conditions to ensure the reliability of the measurement values. Second, we analysed the experimental results according to defect types to establish phased assessment criteria.

Based on the needle–plane electrode system experiment, the results differed with changes in the distance, frequency, temperature, and humidity, even under identical experimental conditions. In summary, the changes in the decibel level according to the measurement distance could be inferred based on the short-range measurement criteria for indoor equipment. In the case of frequency, reliable measurements were performed in the 30–40 kHz band through repeated experiments under different distance, temperature, and humidity conditions. Owing to the differences in the corona discharge characteristics due to temperature and humidity, different values were obtained in the ultrasonic measurements. Therefore, further research is required to obtain detailed correlations of the measurement values with temperature and humidity. Additionally, as the experiment was based only on indoor data, research considering outdoor conditions is necessary.

The comparative analysis of the HFCT and ultrasonic PRPD results based on the defect type confirmed that phased assessment criteria can be devised for measurements using ultrasonic imaging equipment. Typically, phased assessment criteria are divided into good, caution, and abnormal, with the following implications.

- Good: The state wherein no abnormal phenomena are detected when using the equipment.
- Caution: The initial stage of corona discharge, which occurs intermittently or with low severity and requires periodic diagnosis.
- Abnormal: The stage where insulation deterioration has rapidly progressed, which requires immediate replacement.

Considering equipment usage, when no ultrasonic signal source is detected on the imaging screen, the assessment is classified as “good”. When an ultrasonic signal source appears on the imaging screen and corona discharge is detected intermittently or with low decibel levels, the assessment is classified as “caution”. Finally, when corona discharge is continuously detected with high decibel values, the assessment is classified as “abnormal”.

Figure 13 shows a flowchart of the proposed corona discharge assessment criteria for ultrasonic imaging equipment along with the considerations required for assessment based on the experimental results. First, the environmental conditions are evaluated before starting the diagnosis. After diagnosis, the “good” assessment is determined based on the presence of an ultrasonic signal source. The assessment varies depending on whether the ultrasonic signal source occurs intermittently or continuously. If it occurs continuously but a PRPD pattern is not secured, the designation will be “caution”. After securing the PRPD pattern, the decibel level is recalculated by applying the measurement environmental conditions, and the assessment is performed based on the criteria for “caution” and “abnormal”.

The criteria should consider the correlation based on temperature and humidity. Notably, the “abnormal” criterion values differ for each device, an aspect that necessitates further research.

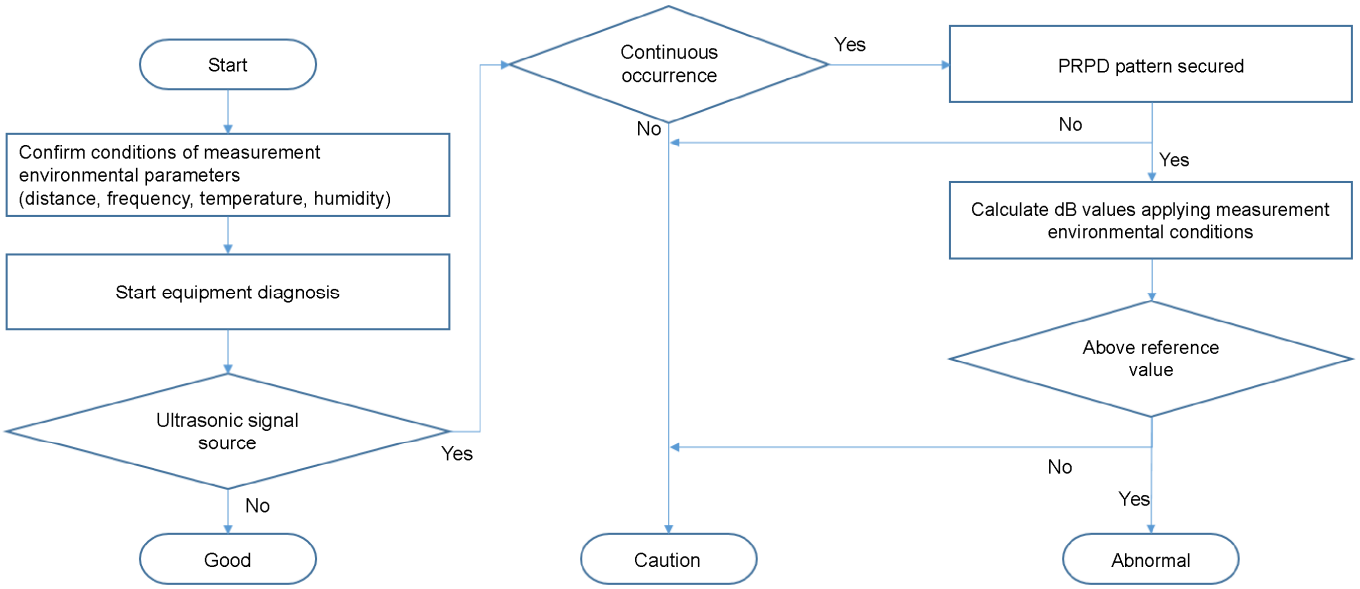

Figure 13. Flowchart of the proposed corona discharge assessment criteria for ultrasonic imaging equipment.

5. Conclusions

This study investigated the measurement technique of ultrasonic imaging equipment for detecting corona discharge in a non-contact manner. First, the basic measurement technique of ultrasonic imaging equipment was established based on distance, frequency, temperature, and humidity. Based on the test results, essential environmental conditions for measurement were suggested by repetitive measurement using a corona electrode. Second, three types of epoxy line–post insulators (simply aged, cracked by accelerated degradation, and artificially damaged on the surface) were prepared and measured to investigate the PD characteristics of the proposed technique for different types of defects. The results of the PD pulse analysis confirmed the differences in the detected PD pulses according to the defect type. These findings will be helpful for determining the defect type of epoxy line–post insulators based on PD pulses.

Unexpected power failure results in economic losses and inconvenience. Therefore, it is crucial to prevent power failures by performing periodic diagnoses in the live-wire state. This paper provides a measurement technique and PD pulse analysis results for an epoxy-insulated line–post insulator to demonstrate the importance of appropriate on-line diagnosis of electrical infrastructure, such as epoxy-insulated line–post insulators, to prevent power failure. In the near future, various types of core components, such as power cable terminations, lightning arrestors, and epoxy insulators, will be tested and propound PD pulse analysis will be performed to enhance the reliability of the electrical network.

Author Contributions: Conceptualization, J.-Y.K., J.-M.P. and B.-W.L.; methodology, D.-J.C.; software, Y.-C.M.; validation, J.-Y.K., J.-M.P. and D.-J.C.; investigation, Y.-C.M.; data curation, Y.-C.M.; writing—original draft preparation, J.-Y.K.; writing—review and editing, J.-M.P. and B.-W.L.; visualization, Y.-C.M.; supervision, B.-W.L. All authors have read and agreed to the published version of the manuscript.

Funding: This work was supported by the Korea Institute for Advancement of Technology (KIAT) and the Ministry of SMEs and Startups (MSS) of the Republic of Korea (No. P0025179).

Data Availability Statement: Not applicable.

Conflicts of Interest: The authors declare no conflict of interest.

References

1. Florkowski, M. Hyperspectral imaging of high voltage insulating materials subjected to partial discharges. *Measurement* **2020**, *164*, 108070. [CrossRef]
2. Rosle, N.; Muhamad, N.A.; Rohani, M.N.K.H.; Jamil, M.K.M. Partial discharges classification methods in xlpe cable: A review. *IEEE Access* **2021**, *9*, 133258–133273. [CrossRef]
3. Xu, Y.; Yu, M.; Cao, X.; Qiu, C.; Chen, G. Comparison between optical and electrical methods for partial discharge measurement. In Proceedings of the 6th International Conference on Properties and Applications of Dielectric Materials, Johor Bahru, Malaysia, 11–15 July 2000; Volume 1, pp. 300–303.
4. da Costa, I.B.V.; Weber, G.H.; Gomes, D.F.; Galvão, J.R.; da Silva, M.J.; Pipa, D.R.; Ozcáriz, A.; Zamarreño, C.R.; Martelli, C.; Cardozo da Silva, J.C. Electric discharge detection and localization using a distributed optical fiber vibration sensor. *Opt. Fiber Technol.* **2020**, *58*, 102266. [CrossRef]
5. IEEE Power Engineering Society; Insulated Conductors Committee; Institute of Electrical and Electronics Engineers; IEEE-SA Standards Board. *IEEE Guide for Partial Discharge Testing of Shielded Power Cable Systems in a Field Environment*; IEEE: Piscataway, NJ, USA, 2007; p. 36.
6. Wang, Y.; Li, X.; Gao, Y.; Zhang, H.; Wang, D.; Jin, B. Partial discharge ultrasound detection using the Sagnac interferometer system. *Sensors* **2018**, *18*, 1425. [CrossRef] [PubMed]
7. Tang, L.; Luo, R.; Deng, M.; Su, J. Study of partial discharge localization using ultrasonics in power transformer based on particle swarm optimization. *IEEE Trans. Dielectr. Electr. Insul.* **2008**, *15*, 492–495.
8. Wang, X.; Li, B.; Roman, H.T.; Russo, O.L.; Chin, K.; Farmer, K.R. Acousto-optical PD detection for transformers. *IEEE Trans. Power Deliv.* **2006**, *21*, 1068–1073. [CrossRef]
9. Kim, Y.; Shong, K. The characteristics of UV strength according to corona discharge from polymer insulators using a UV sensor and optic lens. *IEEE Trans. Power Deliv.* **2011**, *26*, 1579–1584. [CrossRef]
10. Pinnangudi, B.; Gorur, R.S. Quantification of corona discharges on non-ceramic insulators. *IEEE Trans. Dielectr. Electr. Insul.* **2005**, *12*, 513–523. [CrossRef]
11. Bologna, F.F.; Reynders, J.P.; Britten, A.C. Corona Discharge Activity on A String of Glass Cap-And-Pin Insulators under Conditions of Light Wetting, Light Non-Uniform Contamination. In Proceedings of the 2003 IEEE Bologna Power Tech Conference Proceedings, Bologna, Italy, 23–26 June 2003; Volume 3, p. 8.
12. Da Costa, E.G.; Ferreira, T.V.; Neri, E.G.G.; Queiroz, I.B. Characterization of polymeric insulators using thermal and UV imaging under laboratory conditions. *IEEE Trans. Dielectr. Electr. Insul.* **2009**, *16*, 985–992. [CrossRef]
13. Zhou, W.J.; Li, H.; Yi, X.; Tu, J. A criterion for UV detection of AC corona inception in a rod-plane air gap. *IEEE Trans. Dielectr. Electr. Insul.* **2011**, *18*, 232–237. [CrossRef]
14. Xiao, M.; Wen, C. New method to detect insulation on line ultraviolet image method. *High Volt. Eng.* **2006**, *32*, 42–44. (In Chinese)
15. Zang, C.; Zhao, X.; He, S.; Lei, H. Research on Mechanism and Ultraviolet Imaging of Corona Discharge of Electric Device Faults. In Proceedings of the Conference Record of the 2008 IEEE International Symposium on Electrical Insulation, Vancouver, BC, Canada, 9–12 June 2008; pp. 690–693.
16. He, Z.; Zhu, J.; Bian, X.; Shen, B. Experiments and analysis of corona inception voltage under combined AC-DC voltages at various air pressure and humidity in rod to plane electrodes. *CSEE J. Power Energy Syst.* **2021**, *7*, 875–888.